

## Driven Nonlinear Oscillators

Physics 15a Lab - Spring 2013

### *Simple Harmonic Oscillators:*

Simple harmonic oscillators have a linear response to a driving force, and respond at the same frequency. For example the equation of motion for a mass on a spring driven by a sinusoidal force is:

$$m \frac{d^2 x}{dt^2} = -\gamma \frac{dx}{dt} - kx + F_0 \sin \omega t \quad (1)$$

where  $x$  is the displacement,  $t$  is the time,  $m$  is the mass,  $\gamma$  is damping coefficient,  $k$  is the spring constant, and  $F_0$  is the magnitude of the driving force at angular frequency  $\omega$ . The natural frequency  $\omega_0$  of oscillation is given by:

$$\omega_0^2 = 4mk - \gamma^2 \quad (2)$$

with a damping time  $\tau$  given by:

$$\frac{1}{\tau} = \frac{\gamma}{2m}. \quad (3)$$

The displacement  $x$  of a mass on a spring responds to a sinusoidal drive at the drive frequency  $\omega$ , because the equation of motion Eq. 1 is linear in  $x$  so we have:

$$x(t) \propto F_0 \sin \omega t \quad (4)$$

### *Nonlinear Oscillators - Harmonic Generation*

Let's look at a mass on a spring, which is not ideal, and has a nonlinear response with force  $F_{\text{spring}}$  that includes a cubic term:

$$F_{\text{spring}} = -kx - k_3 x^3 \quad (5)$$

The spring responds linearly to small displacements, but gets firmer as the displacement grows.

With sinusoidal drive at frequency  $\omega$ , this nonlinear spring will respond at both the drive frequency  $\omega$ , and at the third harmonic of the drive frequency  $3\omega$ . If one looks at a plot of the response vs. time, the oscillation develops a flat top, where the maximum excursion falls below that for a linear oscillator. The response at the third harmonic is generated by the cubic component of the restoring force. For a sinusoidal displacement  $x_0 e^{i\omega t}$ , the restoring force is given by:

$$F_{\text{spring}} = -kx_0 e^{i\omega t} - k_3 x_0^3 e^{i3\omega t} \quad (6)$$

generating the third harmonic  $3\omega$ . For nonlinearities at high powers  $x^n$ , the spring will generate the  $n$ th harmonic at frequencies  $n\omega$ .

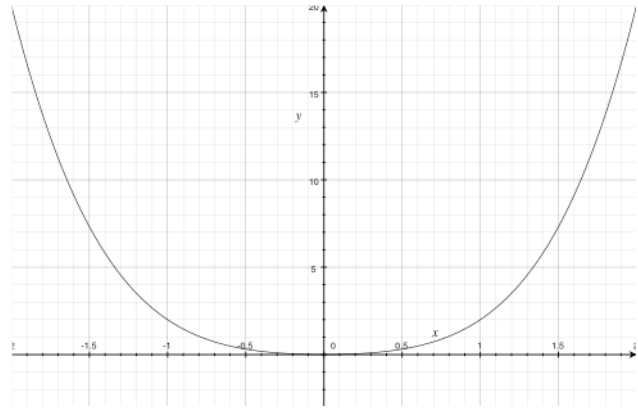


Fig. 1 Potential energy of a hard spring, Eq. 5.

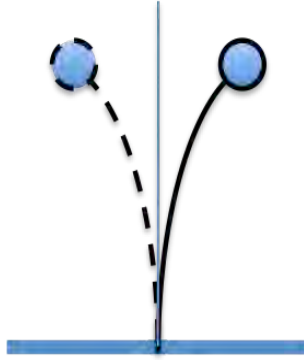


Fig. 2 Duffing oscillator - mass on a springy strip.

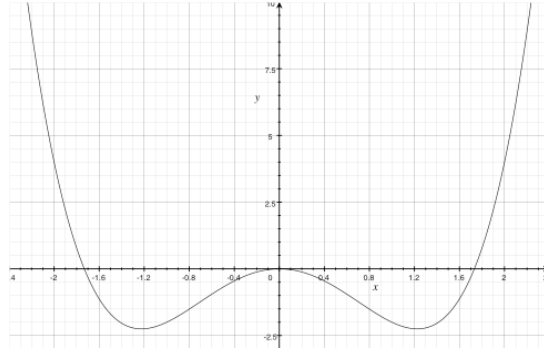


Fig. 3 Potential energy for a Duffing oscillator.

The distinctive sound of a musical instrument is created by the generation of harmonics by its nonlinear response. An instrument that generates a strong third harmonic is an electric guitar with a tube amplifier - popular with Eric Clapton and others. The nonlinear response of the transformers coupling the amplifier to the speaker saturates at high volumes, creating the sound you hear.

### ***Duffing Oscillator - New Types of Response***

New types of motion occur in a Duffing oscillator, shown in Fig. 2. It is an inverted pendulum, constructed by fixing a mass near the end of a springy strip. The force of gravity pulls the mass away from the vertical position at  $\theta = 0$ , either to the left or to the right, and the springy strip provides the restoring force that stops the descent. The potential energy, shown in Fig. 3, has a "W" shape, with a local maximum at  $\theta = 0$ , and two minima, one at  $\theta_+$  and another at  $\theta_-$ .

The equation of motion for the Duffing oscillator can be expressed as two first-order differential equations:

$$\begin{aligned} \frac{d\theta}{dt} &= v \\ \frac{dv}{dt} &= -\gamma v + (k\theta - k_D \theta^3) + F_D \sin \omega t \end{aligned} \quad (8)$$

where  $v$  is the angular velocity  $d\theta/dt$ . Because the time  $t$  appears in the sinusoidal driving force, the equations of motion have three variables:  $\theta$ ,  $v$ , and  $t$ . For simplicity, we let the dimensions of  $\gamma$ ,  $k$ ,  $k_D$ , and  $F_D$  be rad/sec.

**Attractors and Basins of Attraction:** It's interesting to consider the response of a Duffing oscillator without drive ( $F_D = 0$ ). By considering the vector flow ( $d\theta/dt$ ,  $dv/dt$ ) corresponding to the equation of motion at different points  $(\theta, v)$ , shown in Fig. 4, we can understand what happens. If the mass of a simple harmonic oscillator is released, its position will ring down to  $x = 0$ , where the potential energy is a minimum. However, for a Duffing oscillator, the central position  $\theta = 0$  is unstable. If you release the mass near  $\theta = 0$  it will move away and spiral into either the potential well about  $\theta_+$  or into the well about  $\theta_-$  as shown in Fig. 4. The system makes this decision to go right or left, based on whether the initial angle was slightly positive or

negative. The ability to make decisions based on the initial conditions is a characteristic of nonlinear systems - that is why all computers are made of nonlinear elements - switches.

The existence of multiple stable states is common in nonlinear systems - they are called *attractors*. The stable angles at  $\theta_+$  and  $\theta_-$  are attractors for the undriven Duffing oscillator, and it will ring down to one of these two angles. The set of initial conditions that falls to a particular attractor is called its *basin of attraction*.

An important example of a nonlinear system based on attractors and basins of attraction is CMOS logic. The digital states "1" and "0" are each represented by an attractor at a particular voltage " $V_1$ " or " $V_0$ " in the logic circuit. Large voltages (2 to 3 V) representing "1", fall onto the attractor at " $V_1$ ", while a small voltages (0 to 1 V) representing "0" fall onto the attractor at " $V_0$ ". These are the basins of attraction for the attractors representing "1" and "0". The fact that a range of voltages represents each bit of information allows the system to tolerate noise without making mistakes.

### ***Duffing Oscillator - Driven Response***

When driven by a small oscillating force  $F_D \sin \omega t$ , with  $F_D \ll 1$ , the Duffing oscillator will relax either into the well about  $\theta_+$  or the well about  $\theta_-$  and oscillate periodically at the drive frequency  $\omega$  and its harmonics. With periodic drive, the shape of the attractors at  $\theta_+$  and  $\theta_-$  change from a point to a closed loop in the phase space defined by  $\theta$  and  $\dot{\theta}$ , and the mass travels around the loop as long as the oscillating force is supplied.

For larger forces  $F_D > 1$ , the response changes and generates qualitatively new types of behavior, including complicated orbits with periods greater than the drive period  $2\pi/\omega$ , and orbits that are not periodic at all - *chaos* - which appears to be broadband noise. The generation of chaos by simple nonlinear systems is a fascinating topic.

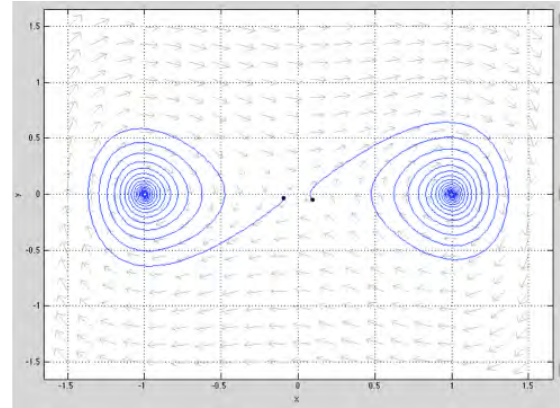


Fig. 4 Vector field for the Duffing equation:  $x' = y$  ;  $y' = -0.1y + x - x^3$ . Trajectories show the existence of two attractors.

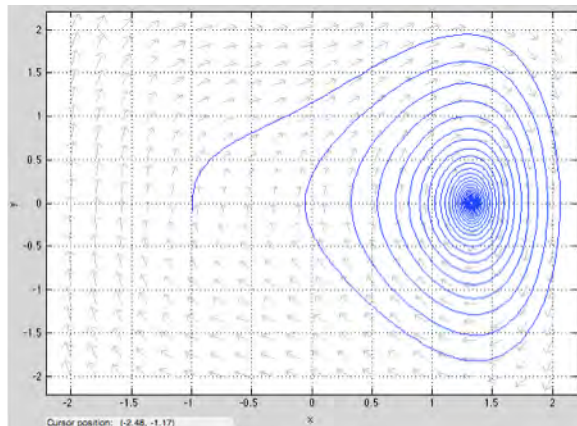


Fig. 5 Vector field and trajectory for forced Duffing equation:  $x' = y$  ;  $y' = -0.1y + x - x^3 + 1$  at fixed drive phase  $\omega t = \pi/2$ .

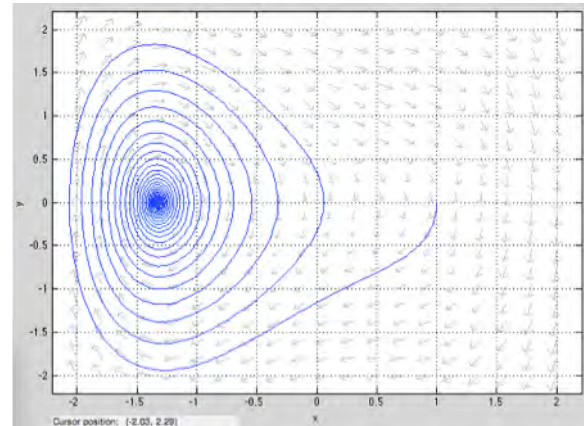


Fig. 6 Vector field and trajectory for forced Duffing equation:  $x' = y$  ;  $y' = -0.1y + x - x^3 - 1$  at fixed drive phase  $\omega t = 3\pi/2$ .

## Chaos

While small driving forces  $F_D \ll 1$  leave the Duffing oscillator in a single well, large forces repetitively move the mass from one well to the other, generating folds in the phase space. This happens because the equation of motion changes in time through the action of the oscillating force  $F_D \sin \omega t$ . To see how this happens, let's look at a series of snapshots of the vector field corresponding to the equation of motion taken at different times for  $F_D = 1$ . At  $\omega t = 0$ , the force is zero, and the vector field diagram (Fig. 4) has two wells of the same size. However at  $\omega t = \pi/2$ , the force  $F_D \sin(\pi/2) = 1$ , and the vector field (Fig. 5), has only the well about  $\theta_+$ . The positive force cancels the well about  $\theta_-$  and enlarges the well about  $\theta_+$ . A quarter cycle later at  $\omega t = \pi$ , the force  $F_D \sin(\pi) = 0$ , falls to zero again, and the two wells reappear, but at  $\omega t = 3\pi/2$  the force  $F_D \sin(3\pi/2) = -1$  reaches a negative peak at -1, and the vector field diagram (Fig. 6) shows only the negative well about  $\theta_-$ , because the well about  $\theta_+$  has been destroyed.

Imagine that you are holding one marble in an egg carton. If you shake the egg carton gently from side to side, the marble will rock back and forth inside the well for one egg. However if you shake it more strongly, so that the marble can move between wells, more complex behavior will occur.

You can numerically solve the Duffing differential equation Eq. 8 using the Apple Grapher application in the Applications/Utilities folder of your Mac. Simply enter the equation, the initial conditions, and the time range into the grapher equation window and press return, as shown here:

$$\frac{d}{dt} \begin{bmatrix} x \\ y \end{bmatrix} = \begin{bmatrix} y \\ -0.1 \cdot y + x - x^3 + 2.4 \cdot \sin t \end{bmatrix}, \begin{bmatrix} x \\ y \end{bmatrix} = \begin{bmatrix} 0 \\ 0 \end{bmatrix}, t=0 \dots 100 \quad (9)$$

where  $x$  is  $\theta$  and  $y$  is  $\dot{\nu}$ . Grapher plots the resulting curve in the  $x$ - $y$  ( $q$ - $\dot{q}$ ) plane, shown in Fig. 7 above for a driving force amplitude  $F_D = 2.4$ .

The trajectory shown in Fig. 7 exhibits *chaos* - instead of following a closed loop, the trajectory wanders through phase space in a complicated pattern that does not repeat in time. In addition, the trajectory is highly sensitive to its starting point - if you move the starting point by a small amount, you'll obtain a very different curve. Using the Grapher application, you can play with the control parameters - the amplitude and frequency of the applied force - to see what types of motion are possible.

Chaotic trajectories are possible, because the vector field corresponding in Eq. 8 changes in time through the sinusoidal drive force, as shown in Figs. 5 and 6. This means that orbits can cross over each other to create a chaotic orbit (Fig. 7). It's the difference between flat highway system with no bridges, and a highway system with overpasses.

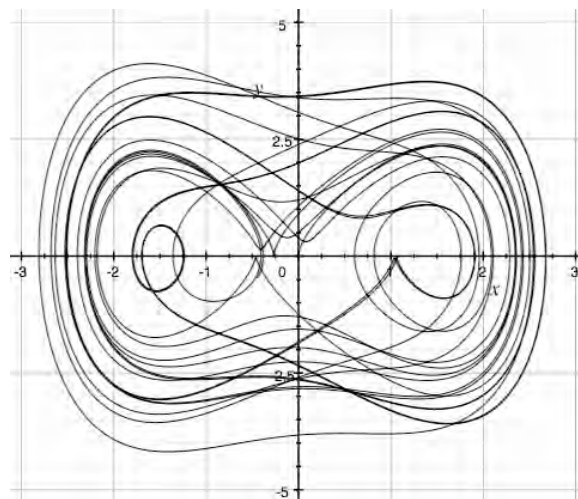


Fig. 7 Chaotic trajectory for Duffing equation with sinusoidal drive (Eq. 9) using the Grapher application ( $x$  is  $\theta$  and  $y$  is  $\dot{\nu}$ ).



### ***Folding in Phase Space***

A common source of nonlinear phenomena such as chaotic orbits, and the period doubling sequence of bifurcations to chaos is folding of orbits in phase space. This is best explained graphically using numerical simulations of a simple nonlinear system called the Rössler model of the Duffing system of equations. Abraham and Shaw (1978) have a great presentation of this topic in *Dynamics: the Geometry of Behavior, Part 2 Chaotic Behavior*.

The equations of motion for the Rössler model are:

$$\frac{dx}{dt} = -y - z \quad (10a)$$

$$\frac{dy}{dt} = x + ay \quad (10b)$$

$$\frac{dz}{dt} = b + z(x - c) \quad (10c)$$

where  $x$ ,  $y$ , and  $z$  are the variables and  $a$ ,  $b$ , and  $c$  are control parameters. The only nonlinearity is the  $zx$  product in Eq. 10c.

Solutions of the Rössler equation collapse onto an attractor, after an initial transient. The geometry of this attractor is illustrated in Fig. 8 and a typical trajectory is shown in Fig. 9. Each cycle around the attractor folds once onto itself, and stretches laterally to recover the same width. The process is like making puff pastry that originally consists of one layer of butter enclosed by one layer of bread dough. One makes additional layers by folding the pastry dough onto itself, and rolling it out to return to the same shape. Ten folds gives  $2^{10} = 1024$  layers - called *millefeuille* in French.

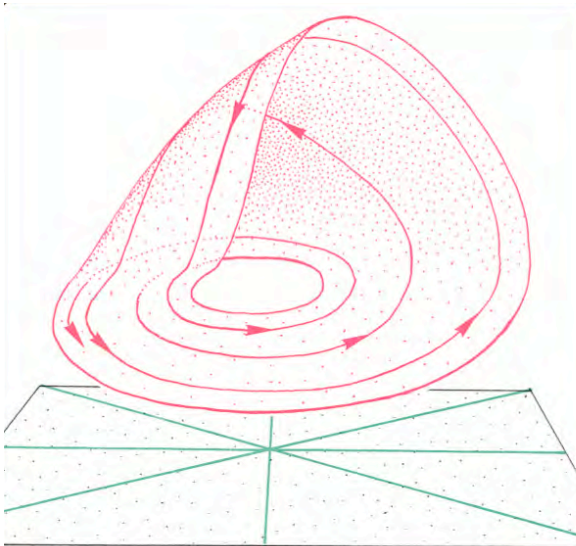


Fig. 8 Drawing of the attractor band for the Rössler equations (Eq. 10), showing one particular orbit. Each time around the band folds once onto itself, and the orbits diverge laterally (Abraham and Shaw 1978).

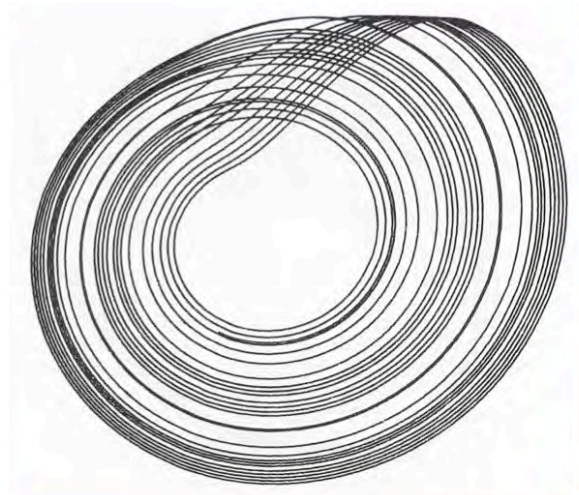


Fig. 9 Chaotic trajectory in the Rössler attractor, top down view of Fig. 8 (Abraham and Shaw 1978)

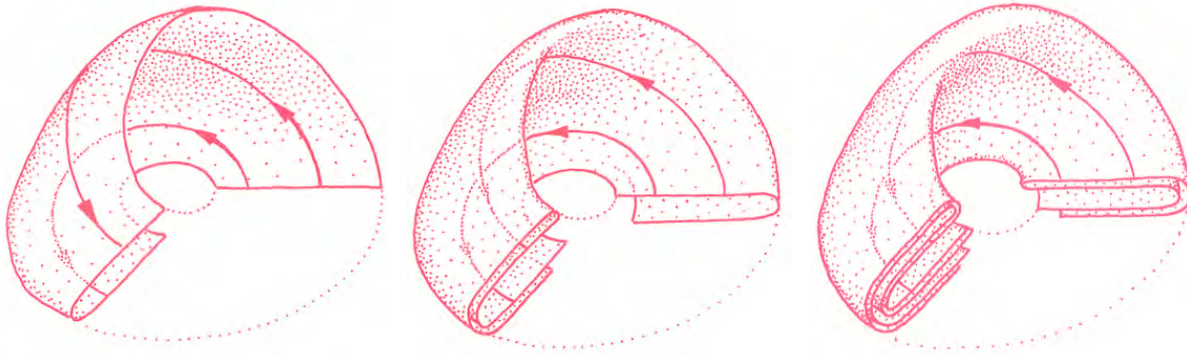


Fig. 10 Repetitive folding of the Rössler band produces 2, 4, and 8 folds, and eventually infinitely many folds, to create a *strange attractor* with a fractal dimension (Abraham and Shaw 1978).

The effect of a single fold on orbits in the Rössler attractor is shown in the left panel of Fig. 10: the fold mixes the order of two orbits in the initial sheet. In addition, the width of the sheet doubles during each fold to return to its initial value. As a consequence, the separation between two nearby trajectories diverges exponentially in time. The combination of mixing and exponential sensitivity to initial conditions is a defining characteristic of chaotic orbits that leads to the unpredictability of their solutions.

### ***Strange Attractors***

Repetitive fold of the Rössler band creates an attractor with infinitively many folds. Figure 10 illustrates how one fold produces 2 layers, 2 folds give  $2^2 = 4$  layers, and three folds give  $2^3 = 8$  layers. This folding process continues indefinitely and the number of layers increases exponentially in time - for  $n$  folds we get  $2^n$  layers. The resulting Rössler attractor has infinitely many layers and a dimensional that is a *fractal*, not an integer. It is called a *strange attractor* for this reason. An example of fractal is a tree, where a single branch creates two smaller branches, which each create two twigs, and so on.

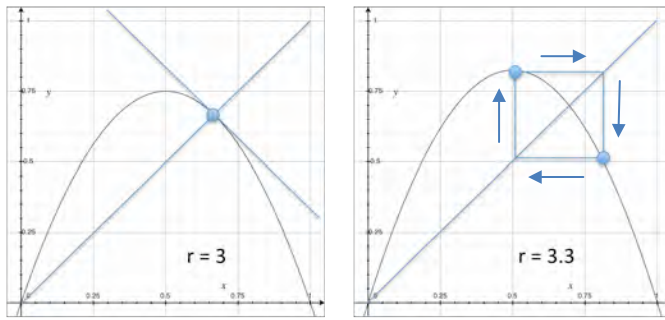


Fig. 11 Logistic map (Eq. 11) plotting  $x_{n+1}$  vs.  $x_n$  the upward sloping blue line has slope 1. For strength  $r = 3$  the attractor is a single point, and the system is critical because the tangent slope is -1. At larger  $r = 3.3$  the attractor period doubles to two points, which alter back and forth every other cycle.

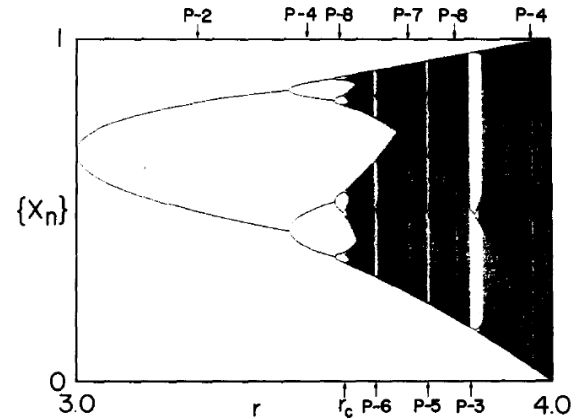


Fig. 12 Period doubling cascade to chaos for the logistic map, showing the attractor values  $\{x_n\}$  vs. strength  $r$ . (Crutchfield et al. Phys Rep **192**, 45 (1982)).

### Period Doubling Cascade to Chaos

A lot can be learned about the effects of folding on dynamics by considering the simple *logistics map*, shown in Fig. 11, which maps the value of the variable  $x_n$  before the fold to the position  $x_{n+1}$  after the fold:

$$x_{n+1} = rx_n(1 - x_n) \quad (11)$$

where the values of the variable are bounded between  $x_n = 0$  and  $x_n = 1$ . Sometimes this is called the predator-prey map, which describes how the number  $x_n$  of predators changes from generation to generation. With few cats and many mice, the number  $x_n$  of cats grows. They eat more mice, and eventually the number of cats becomes too large for all of them to be fed, and their number drops.

Feigenbaum (1978) realized that the logistic map provides a period-doubling route to chaos. Figure 11 shows how this occurs. For relatively 'weak' map with  $r < 3$ , the map has a single point attractor, as shown in the left panel, at which  $x_{n+1} = x_n$ . A critical strength occurs at  $r = 3$ , where the tangent slope reaches -1. For larger a bifurcation of the attractor into a two point limit cycle occurs, as shown on the right - the arrows indicate how one point passes to the other in a period of two cycles.

Plotting the points  $\{x_n\}$  of the attractor vs. the strength  $r$  of the logistic map (Fig. 12), we find a period doubling route to chaos in which the period goes through the sequence 1 - 2 - 4 - 8 - 16 - 32 ... At a universal value  $r = 3.59687$  the attractor becomes chaotic, and as  $r$  continues to increase, the width of the chaotic band increases, with some locked windows. Eventually, for  $r = 4$  the chaotic bandwidth covers the full range of  $x_n$  from 0 to 1, and the map acts as a random number generator.

The period doubling cascade to chaos is commonly observed in nonlinear systems, because can occur whenever a smooth fold is created in the attractor, as observed in the Rössler attractor shown in Figs. 8, 9, and 10.

## Driven Damped Pendulum

A periodically driven damped pendulum is model for many systems including phase locked loops that detect FM radio signals, superconducting Josephson junction detectors of RF radiation, and mechanical oscillators of other types. While a driven pendulum acts like a simple harmonic oscillator when the bob is nearly vertical, it displays a rich variety of nonlinear phenomena at higher angles  $\theta$ , including a period doubling cascade to chaos, frequency locking at fractional modes  $\omega/\omega_o = n/m$ , where  $n$  and  $m$  are integers, and free running modes, where the bob repeatedly swings over the top. It's interesting to investigate some of the phenomena that can occur.

The equation of motion for a driven damped pendulum is given by:

$$\frac{d\theta}{dt} = v \quad (12a)$$

$$\frac{dv}{dt} = -\frac{\xi}{I}v - \frac{\Gamma_g}{I}\sin\theta + \frac{\Gamma_o}{I}\sin\omega t \quad (12b)$$

where  $\theta$  is the angle from vertical,  $v$  is the instantaneous angular velocity,  $\xi$  is the damping coefficient,  $\Gamma_g$  is the amplitude of the torque from gravity, and  $\Gamma_o$  and  $\omega$  are the amplitude and the angular frequency of the driving torque. At small angles and light damping, the natural resonant frequency is  $\Omega_o = (\Gamma_g/I)^{1/2}$ .

For small drive amplitudes and light damping, the driven pendulum acts like a simple harmonic oscillator, because the torque due to gravity is simply proportional to the angle. However, for larger drive amplitude, the pendulum swings to higher angles, and it can even swing over the top to generate running modes to continue to rotate in one direction. These new nonlinear responses are interesting, and they are important, because the equation of motion for a driven pendulum is the same as the equations that describe the operation of a phase-locked loop in electronics, and for a superconducting Josephson junction.

The nonlinear response of a driven pendulum has been examined by D'Humieres *et al.* (1982) and others. At frequencies below the natural frequency  $\Omega_o$ , the pendulum generates new modes of behavior as shown in the 'phase diagram' in Fig. 12 vs. drive frequency and drive amplitude. These include phase locked modes, both fixed ( $n = 0$ ), free running ( $n > 1$ ) with  $n$  additional rotations per drive cycle, and phase locked modes with more complex locking ratios which generate  $p/g$  additional rotations per cycle where  $p$  and  $g$  are two integers. In addition, at large drive the pendulum generates chaotic (intermittent) responses and broadband noise.

To understand the nature of these new nonlinear types of oscillation, it's very useful to make phase space portraits of their trajectories

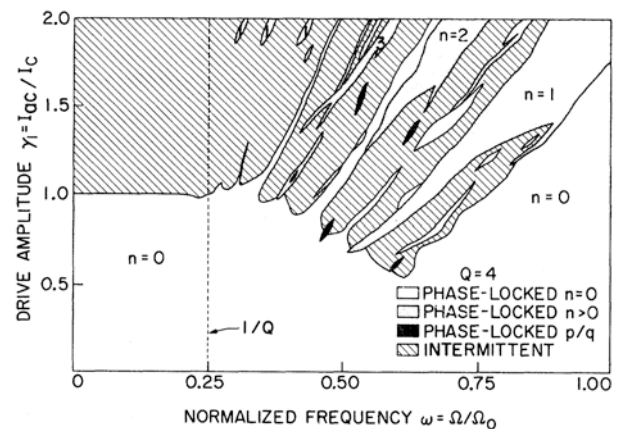


Fig. 12 Phase diagram for a sinusoidally driven damped pendulum with natural frequency  $\Omega_o$  quality factor  $Q = 4$ . Running modes add  $2\pi n$  radians per drive cycle. (D'Humieres et al. 1982).



in the  $v = d\theta/dt$  and  $\sin \theta$  phase space. Using  $\sin \theta$  instead of  $\theta$ , allows one to study the behavior of running modes easily. Figure 13 shows the evolution of the system as the normalized drive amplitude  $\gamma_1$  is increased. For small drive ( $\gamma_1 = 0.46$ ) the trajectory is a simple loop. At a slightly larger drive ( $\gamma_1 = 0.50$ ), symmetry breaking occurs, followed by period doubling ( $\gamma_1 = 0.52$ ), and chaotic oscillations ( $\gamma_1 = 0.54$ ). Nonlinear behavior like this is observed at many combinations of drive frequency and amplitude - you can use the phase diagram shown in Fig. 12 as a guide.

Digital simulations of the driven pendulum can be carried out using the Grapher application. Simply enter a normalized version of the equation of motion:

$$\frac{d\theta}{dt} = v \quad (13a)$$

$$\frac{dv}{dt} = -\frac{1}{Q}v - \sin \theta - \gamma_1 \sin \omega t \quad (13b)$$

You can explore the behavior using different initial conditions - the application will generate phase portraits of the solutions, such as those shown in Fig. 12.

$$\frac{d}{dt} \begin{bmatrix} x \\ y \end{bmatrix} = \begin{bmatrix} y \\ -0.25 \cdot y - \sin(x) - 0.85 \sin(0.67 \cdot t) \end{bmatrix}, \begin{bmatrix} x \\ y \end{bmatrix} = \begin{bmatrix} 0 \\ 0 \end{bmatrix}, t=0 \dots 100$$

Running the solution gives the phase portrait shown below in Fig. 13.

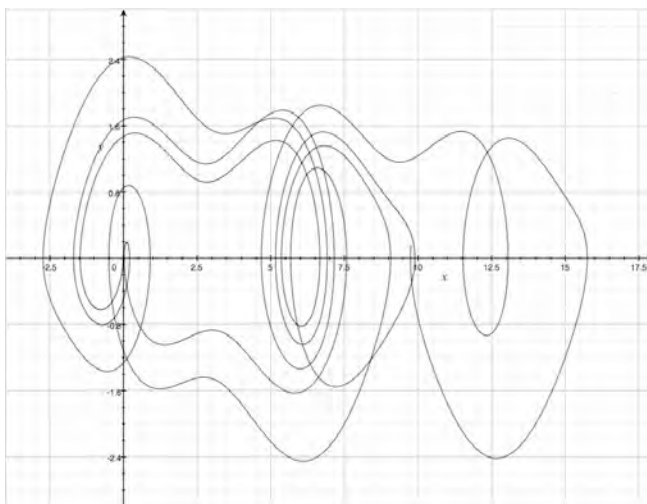


Fig. 13 Grapher solution of the driven damped pendulum with  $Q = 4$ , and drive amplitude 0.85 and drive frequency 0.67, using the equation above.

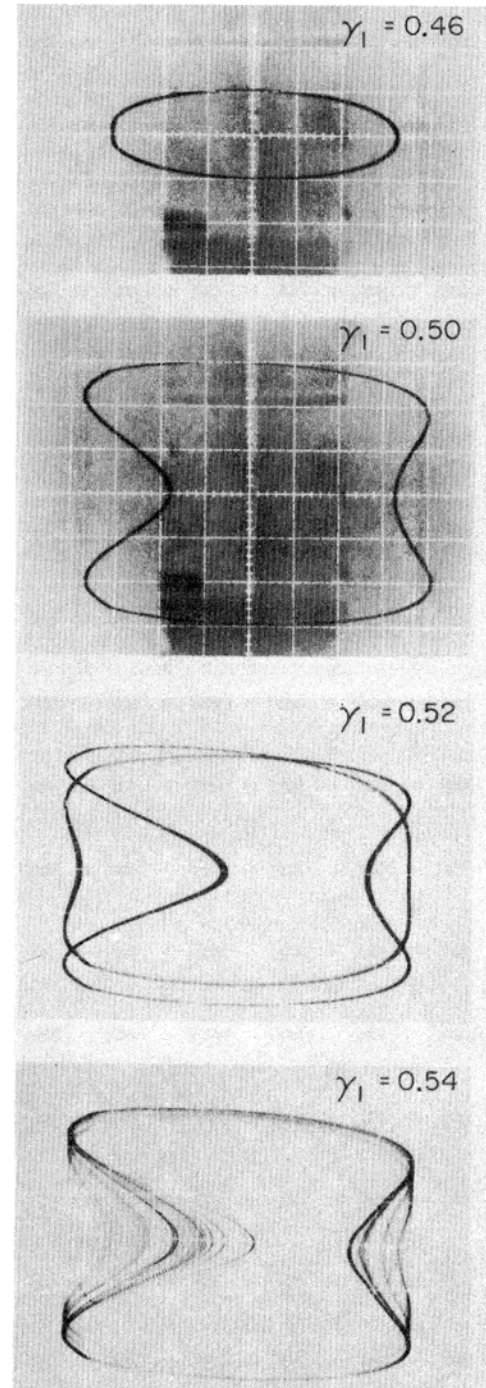


Fig. 12 Evolution of phase space portraits ( $v$  vs  $\sin \theta$ ) for increasing normalized drive amplitude  $\gamma_1$  at the drive frequency  $\omega = 0.67 \Omega_0$ .

## References

R.H. Abraham and C.D. Shaw, *Dynamics the Geometry of Behavior*, 4th Edition, (Ariel Press, 2005).

M. Feigenbaum, J. Stat. Phys. **19**, 25 (1978).

D. D'Humieres, M.R. Beasley, B.A. Huberman, and A. Libchaber, "Chaotic states and routes to chaos in the forced pendulum," Phys. Rev. B **26**, 3483 (1982).

S.H. Strogatz, *Nonlinear Dynamics and Chaos*, (Westview Press, 1994).